Proceedings of ALGORITMY 2000
Conference on Scientific Computing, pp. 151–156

ROLLING CONTACT WITH INERTIA AND FRICTION

DIRK LANGEMANN*

Abstract. The phenomenon of rolling is an essential part of the simulation of vehicles's behaviour, the modelling of wear phenomena and the discussion of security aspects of transport.

We describe a visco–elastic body rolling on a support by a free time–dependent boundary–value problem with NEUMANN boundary conditions. Searching for characteristic effects, we assume a simple geometry, i. e. a nearly round wheel tyre rolling on a plane support, but we consider a formulation in EULERian coordinates.

The model contains a driving or breaking moment acting on the axle, and it does not require any given rigid body slip. On the contrary, we get it as an output of the model. Finally, we want to investigate the stability of the quasi–stationary solution of the problem and show some extracts from the behaviour of a rolling wheel.

Key words. rolling contact, free boundary–value problem, hyperbolic partial differential equation, friction

AMS subject classifications. 65Cxx, 65Nxx, 73T05

1. Introduction. The numerical simulation of rolling is an essential input for many applications, in particular in the modelling of vehicle dynamics. Real rolling is never perfect, i. e. it is always a sum of pure rolling and a sliding motion of the wheel or a general rolling body. Furthermore, we find a contact patch of considerable extension between the wheel and its support. The effects within the contact patch influence the dynamical behaviour of the system, the amount of dissipated energy and the resistance to wear and damage.

The classical literature about rolling contact in engineering sciences, cf. [6] and [7], discusses mainly a quasi–stationary rolling contact. They regard an elastic body moving with a constant speed v and a constant rotational velocity ω over the support. All effects within the contact patch are described in a coordinate system moving with the same speed v, and the displacements and forces in the contact area are assumed to be constant in the moving coordinate system. The fact founded in [3] that a driving wheel causes an adhesion zone at the incoming border of the contact patch, plays an important role in the named literature.

This simplification makes it impossible to discuss the stability of the solution or to simulate acceleration or breaking of the vehicle. Observed stick/slip phenomena cannot be modelled, too. In particular, the rotational speed acts as an input, and hence $\omega(t)$ cannot be simulated. Also, other approaches like [8] using elasticity of finite deformations, [1] using sophisticated descriptions of a non–ideal support of the rolling wheel, or [9] and [12] developing effective techniques to handle quasi–stationary contact, cannot circumvent these problems.

Those are the reasons why we will formulate a time–dependent free boundary–value problem for the simulation of rolling contact. The basic equations are presented in Sec. 2 and they are solved by finite element methods in Sec. 3. Results and first parameter studies are presented in Sec. 4. There, the *fundamental behaviour* of an elastic wheel in rolling contact is shown by hands of an example.

*Department of Mathematics, University of Rostock, D–18051 Rostock, Germany, (lgm@alf.math.uni-rostock.de).

A critical input into the simulation of rolling contact is friction. Two particles in contact – one at the wheel surface and the other at the support – have a relative velocity s to each other. Having no better alternative, the classical COULOMB's friction law is used, cf. [10]. We will accept this unsatisfactory assumption in this paper and let the influence of the friction law to further investigation.

2. Basic equations. The reference configuration of the wheel is called $\Omega \subset \mathbb{R}^3$. The particles are $X \in \Omega$ and they are mapped by $\chi : (X,t) \mapsto x(t)$ to the points $x(t)$ of the time–dependent deformed configuration $\chi(\Omega,t)$. Due to the physical backround we can assume smoothness like e. g. $\chi \in C^2(\Omega \times [0,\infty))$. We denote the time derivative by $\dot{x}(t)$ and the nabla operator with respect to the deformed configuration by ∇_x.

The stress tensor may be $L_x(x)$ and we will later refer to the question of what kind L_x is. We get the free boundary–value problem with NEUMANN boundary conditions

$$\begin{array}{rcll} \varrho(x)\cdot\ddot{x}(t) & = & \nabla_x \cdot L_x(x(t)) + f(x,t) & \text{in} \quad \chi(\Omega,t)\,, \\ p(x,t) & = & L_x(x(t))\cdot n(x,t) & \text{on} \quad \partial\chi(\Omega,t) \end{array} \tag{1}$$

where p is the outer force density, f is the inner force density and $n(x,t)$ is the outer normal at the point $x \in \partial\chi(\Omega,t)$ on the boundary of the deformed configuration and at the time t. The density of the material is $\varrho(x)$. For completation of Eq. (1) we need initial conditions $x(0) = x_0$ and $\dot{x}(0) = \dot{x}_0$.

The inner forces consist in the gravity and in the inner damping of the visco–elastic material $f_d(x,t) = c\nabla_x \cdot L_x(\dot{x}(t))$ with the damping coefficient c, cf. [5]. We will not write this term explicitely into our equations but we will keep it in mind and use it in the example following in Sec. 4.

The outer forces are the weight F_G of the vehicle acting on the axle and a driving or breaking moment M (resp. B) acting on the axle too, which may depend on time or on the rotational velocity of the wheel. Both integrated quantities need to be applied in a suitable manner on that part of the boundary $\partial\chi(\Omega,t)$ touching the axle. We get the pressure p_g from the splitted F_G and the force density m from the moment M. A respective longitudinal force F_Z is acting on the axle of a tracked wheel.

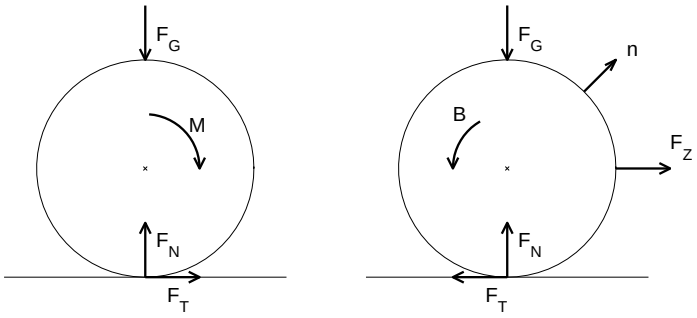

FIG. 1. *integrated forces of a driving wheel and a tracked wheel*

Furthermore, the contact with the support S produces a normal pressure p_n. Due to friction, it results in a tangential pressure p_t. So, we get $p = p_g + m + p_n + p_t$. The integrated pressures, i. e. the forces are shown in Fig. 1.

The distance of $x(t)$ to the rigid or deformable support S may be $d(x,t)$. The point x is in contact to S if $d(x,t) = 0$, in this case we name the point $y = x \in S$ on the support. The relative velocity of these points to each other is $s(x,t) = \dot{x}(t) - \dot{y}(t)$. If S is rigid, then $\dot{y}(t) = 0$ and $s(x,t) = \dot{x}(t)$.

Now, the following contact condition, cf. [5], has to be fulfilled at each point $x \in \partial\chi(\Omega, t)$ and every time instant t

$$d(x,t) \cdot p_n(x,t) = 0 \quad \text{and} \quad p_n(x,t) \cdot n(x,t) \leq 0\,. \tag{2}$$

The tangential forces are governed by COULOMB's law and it holds with the frictional coefficient κ

$$p_t(x,t) = -\kappa \frac{s}{|s|} |p_n| \quad \text{if} \quad s \neq 0 \quad \text{(sliding)}, \tag{3}$$

$$|p_t(x,t)| \leq \kappa |p_n(x,t)| \quad \text{and} \quad p_t(x,t) \cdot n(x,t) = 0 \quad \text{if} \quad s = 0 \quad \text{(sticking)}\,. \tag{4}$$

Most of the literature mentioned above focus on the quasi–stationary solution of the system (2), (3) and (4). The integral over the normal pressure p_n is the counteracting force to F_G and thus, Eq. (2) has the form of a FREDHOLM's integral equation of the first type. Therefore, some difficulties occur while solving this subproblem. We circumvent this problem by investigating the complete system in Sec. 3.

3. Numerical technique. In this section modifications are introduced which make the numerical handling of Eq. (1) easier or only then possible. Let us give a weak formulation of the boundary–value problem (1), $\varphi(x) \in C^1$ is a test function. We get

$$\begin{aligned}(\varrho\ddot{u}, \varphi)_{\mathcal{L}} &= (\nabla_x \cdot L_x(x(t)), \varphi)_{\mathcal{L}} + (f, \varphi)_{\mathcal{L}} \\ &= -\int_{\chi(\Omega,t))} L_x(x(t)) : \nabla_x \varphi(x)\, dx + \int_{\partial\chi(\Omega,t))} p(x,t) \cdot \varphi(x)\, dx + (f, \varphi)_{\mathcal{L}}\end{aligned} \tag{5}$$

with the scalar product $(.,.)_{\mathcal{L}}$ in $\mathcal{L} = H^0(\chi(\Omega, t))$.

We have not yet specified the tensor L_x. The preferable choice would be the first CAUCHY stress tensor $T^{\chi}(x(t))$. In that case the numerical handling of the implicite and non–linear system (1),...,(4) with a reasonable accuracy would be more than actual computer technique can cope with.

On the other hand, the second PIOLA–KIRCHHOFF stress tensor $\Sigma(X)$ is much easier to handle, cf. [4], but it is impossible to model contact completely in undeformed coordinates X, see [11]. Shortly speaking, that is because the outer normal of the reference configuration is not orthogonal to the tangent of the contact patch.

We use the fact $T^{\chi}(x(t)) = |F(X)|^{-1} F(X)\Sigma(X)$ for $x(t) = \chi(X,t)$ with the deformation gradient $F(X) = \nabla\chi(X)$. It is known, that $\Sigma(X)$ can be well approximated by $\sigma(X,u) = \lambda I \nabla \cdot u(X) + \mu[\nabla u(X) + \nabla u(X)^{\mathrm{T}}]$ with the LAMÉ coefficients λ and μ if $u(X)$ is a small deformation, i. e. $F(X) \approx I$ for all $X \in \Omega$.

Furthermore, a rigid body transformation of an isotropic body effects no strain and thus no stress. We divide the map χ into a rigid body transformation η and a small deformation u with $\chi(X,t) = \eta(X,t) + u(X,t)$. With the rotational matrix $D(\alpha)$ for the generalized angle $\alpha \in \mathbb{R}^3$, we find by

$$(\bar{z}(t), \bar{\alpha}(t)) = \arg \min_{z,\alpha \in \mathbb{R}^3} \int_{\Omega} \| D(-\alpha)[\chi(X,t) - z] \|_2 \, dX \tag{6}$$

the coordinates $\bar{z}(t), \bar{\alpha}(t)$ of the rigid body transformation $\eta : X \mapsto D(\bar{\alpha})X + \bar{z}$ minimizing the norm of the elastic deformation u for fixed time. In Eq. (6), the coordinates $\bar{z}(t)$ and $\bar{\alpha}(t)$ are computed by taking the average over all particles.

We approximate $\Sigma(X) \approx \sigma(\eta X, u)$ and finally, we use

$$L_x(x(t)) = |F(\eta X(x))|^{-1} F(\eta X(x)) \sigma(\eta X(x), u)\,. \tag{7}$$

Now, we can reformulate system (5) in undeformed coordinates X of the reference configuration while still using the forces depending on the deformed configuration by $f(X,t) = f(x(t),t)$ and so on.

The discretization of system (5) using the simplification (7) is standard finite element method. We choose test functions $\varphi_i(X) \in C^1(\Omega)$ with $i = 1,\ldots,N$ and write $u(X,t) = \sum_{i=1}^{N} u_i(t)\varphi_i(X)$. In the easiest case where the deformation gradient $F \approx I$ in Eq. (7) is regarded as neglectable and the density ϱ is assumed to be constant[1], we get the system of ordinary linear differential equations ($j = 1,\ldots,N$)

$$\varrho \sum_{i=1}^{N} \ddot{u}_i \cdot (\varphi_i, \varphi_j)_{\mathcal{L}} = \sum_{i=1}^{N} u_i \int_\Omega L\varphi_i : \nabla\varphi_j \, dX + \int_{\partial\Omega} p \cdot \varphi_j \, dX + (f, \varphi_j)_{\mathcal{L}}\,. \tag{8}$$

The great advantage of the linear system is the possibility to compute stiffness, mass and damping matrices in a preprocessing. The influence of this linearization is assumed to be lower than the incertainty of COULOMB's law (3), (4).

Evidently, we get a non–linear system of ordinary differential equations if the influence of $F(X)$ is taken into account. It is enormously more time consuming than the linear system (8) but feasable. This influences the numerical solution but does not change the fundamental behaviour presented in Sec. 4.

A next problem consists in the handling of condition (4) which does not express the tangential traction p_t as a funtion of the normal pressure p_n but as an inclusion. In [11] a class of mechanical systems including real rolling is given for which the influence of a smooth regularization of a discontinuous and non–single valued friction law decreases with the order of the regularization parameter ν. Instead of Eqs. (3) and (4) we use the regularization

$$p_t(x,t) = -\frac{2\kappa}{\pi} \frac{s}{|s|} |p_n(x,t)| \arctan\left(\frac{|s|}{\nu}\right) \tag{9}$$

for all s, cf. [2]. With Eq. (9), the system (8) is completed and can be solved by standard methods.

4. Results. A very simple example is presented here, it has been choosen to demonstrate fundamental effects shortly.

We have used a plane WINKLER–bedding as support S, i. e. elastic in vertical direction and undeformable in the tangential directions. A soft wheel tyre with small inner damping was chosen for the numerical experiments

We have taken the initial conditions $x_0 = 0$ and $\dot{x}_0 = 0$. The numerical simulation contains two steps, where step 1 was done to get realistic initial conditions for step 2 :

1. The wheel falls onto its support by its own gravity, and then the vertical load F_G is applied. After this step, the wheel lays stationarily on the support.
2. The wheel is accelerated by a driving moment M.

In Fig. 2, the longitudinal rigid body motion $\bar{z}_1(t)$ of a driven wheel is shown. Here, nearly whole the driving moment is consumed to overcome the friction force. We have got a nearly linear motion of the centre of gravity of the wheel – comparable

[1] This assumption can be well accepted for standard elastic material like steel or aluminium.

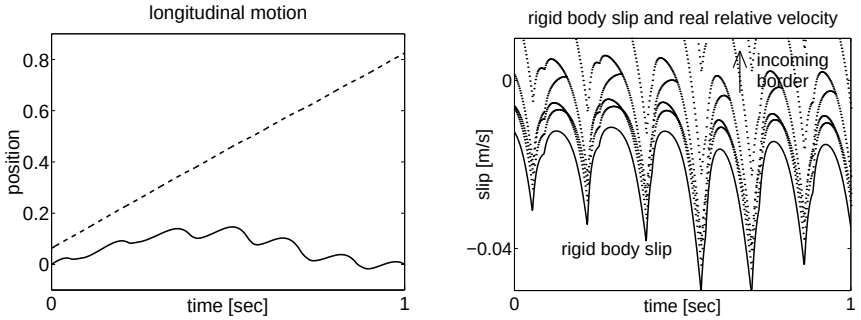

FIG. 2. *position of wheel's centre of gravity and its deviation from ideal linearity; slip*

with a vehicle going slowly with a nearly constant speed of $v \approx 0.75\,\mathrm{m/s}$. The twenty–time exaggerated deviation from a steady motion is shown in the lower part of the figure.

Although, the speed is very slow and the deviation from a steady motion is small, vibrations occur in the contact zone. The right graphic shows the rigid body slip $\bar{s}$ calculated from the coordinates in Eq. (6), i. e. the slip a rigid body would effect moving with the mean velocity. The points above $\bar{s}$ show the relative velocities of selected points near the contact zone. Due to the low speed v they are slower than $\bar{s}$, but in general they are not. The vibrations are enforced with higher speed. The wheel does not tend to a quasi–stationary motion, but it vibrates in a complex manner. Further, the model provides the rigid body slip $\bar{s}$ as an output.

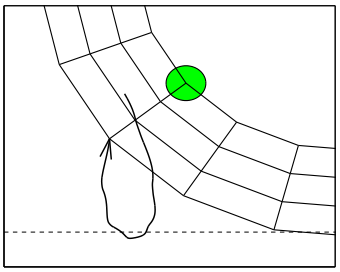

FIG. 3. *trajectory of a point after contact*

The sectional view in Fig. 3 shows the motion of a single particle on the boundary in detail. It has just before undergone contact with the support. It is visible that the wheel spins and effects a negative slip $s < 0$. The particle slides backwards while it is in contact with the support. Again, its vibration is remarkable and the assumption of a quasi–stationary rolling is questionable. The dashed line in Fig. 3 shows the position of the undeformed support. Due to the deformable support the wheel seems to dip into.

A next question is the relation between the integrated normal and tangential forces. Such an integrated friction law would be needed for a much easier multi–body description of a rolling system. In Fig. 4 both forces are shown in a plot.

In this situation of rolling, the tangential force is nearly saturated with the frictional coefficient $\kappa = 1$. The loops inwards the unsaturated frictional force characterize stick phases and the intervals where the tangential force is nearly saturated

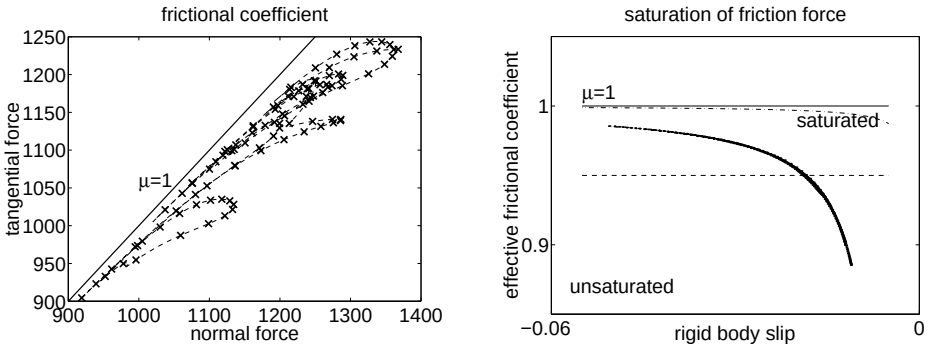

FIG. 4. *normal force vs. tangential force; effective frictional coefficient vs. rigid body slip*

characterize slip phases.

In the right plot of Fig. 4, the effective frictional coefficient $\bar{\mu}(\bar{s}) = F_T/F_N$ is shown. We remark a strong dependence on $\bar{s}$. For comparison, the relation (9) with the used parameter $\nu = 10^{-4}$ is given by the dashdot line. The point–wise friction law has been integrated to a relation between F_T, F_N and $\bar{s}$.

As seen in Figs. 2, 3 and 4, the fundamental behaviour of a visco–elastic rolling body is dominated by vibrations which are in general not periodical. This leads to the suggestion that the standard assumption founded in [3] is to discuss.

The proposed model simulates stick/slip effects. It contains the possibility of a motion with nearly constant speed. Due to damping the model includes the case that a wheel finishes rolling and stays left by itself in the case of $M = B = 0$ and $F_Z = 0$. Further results will be presented in the conference communication.

REFERENCES

[1] J. BIRKEDAL NIELSEN, *New developments in the theory of wheel/rail contact mechanics*, TU of Denmark, dissertation, IMM-PHD-1998-51, Lyngby, 1998

[2] R. BOGACZ, K. FRISCHMUTH, AND D. LANGEMANN, *Numerical analysis of a mechanical model including discontinuous friction forces* in Simulacja w badaniach i rozwoju, conference proceeding to Jelenia Góra, october 5–7, 1998, Warsaw, 1999

[3] F. W. CARTER, *On the action of a locomotive driving wheel*, Proceedings of the Royal Society of London, A112, pp. 151–157, 1926

[4] P. G. CIARLET, *Mathematical Elasticity*, vol. 1: Three dimensional theory of elasticity, Studies in Mathematics and its Applications 20, Elsevier Science Publishers, Amsterdam, 1987

[5] G. DUVAUT, AND J. L. LIONS, *Inequalities in Mechanics and Physics*, Berlin, 1976

[6] K. L. JOHNSON, *Contact Mechanics*, University Press, Cambridge, 1985

[7] J. J. KALKER, *Three–Dimensional Elastic Bodies in Rolling Contact*, vol. 2 of Solid Mechanics and its Applications, Kluwer Academic Publisher, Dordrecht, 1990

[8] N. KIKUCHI, AND J. T. ODEN, *Contact Problems in Elasticity*, SIAM Philadelphia, 1988

[9] K. KNOTHE, AND HUNG LE–THE, *A method for the analysis of the tangential stresses and the wear distribution between two elastic bodies of revolution in rolling contact*, Int. J. Solid Structures vol. 21, No. 8, pp. 889–906, 1985

[10] I. V. KRAGELSKI, *Friction and Wear*, Butterworth Washington DC, 1965

[11] D. LANGEMANN, *Numerische Analyse abrasiv verschleißender mechanischer Systeme* (Numerical analysis of abrasively wearing mechanical systems), Fortschrittberichte 12.392, VDI–Verlag Düsseldorf, 1999

[12] U. NACKENHORST, *An Adaptive Finite Element Method to Analyse Contact Problems*, Computational Mechanics Publications, pp. 241–248, Southampton/Boston, 1995